Malaysian Journal of Analytical Sciences (MJAS)
Published by Malaysian Analytical Sciences Society

METHYLENE BLUE AND METHYL RED FROM PINEAPPLE PEEL–BASED BIOSORBENT FOR MASS TRANSFER SIMULATION AND STATISTICAL APPROACH

(Penggunaan Metilena Biru dan Metil Merah sebagai Biosorben Berbahan Kulit Nanas dalam Simulasi Pemindahan Jisim dan Pendekatan Statistik)

Nur Ayshah Rosli[1*], Mohd Azmier Ahmad[1], and Teh Ubaidah Noh[2]

[1]*School of Chemical Engineering, Engineering Campus, Universiti Sains Malaysia, 14300, Nibong Tebal, Penang, Malaysia*
[2]*Institute of Bioproduct Development, Universiti Teknologi Malaysia, 81310, Skudai, Johor, Malaysia*

[*]*Corresponding author: chnurayshah@usm.my*

Received: 11 August 2023; Accepted: 3 October 2023; Published: 29 December 2023

Abstract

The study focused on the utilization of pineapple peel activated carbon (PineAC) biosorbent, produced through a low–cost and environmentally friendly method, for the adsorption of methylene blue (MB) and methyl red (MR) dyes. PineAC was characterized using various techniques such as surface analysis, scanning electron microscopy (SEM), energy–dispersive X–ray (EDX), and Fourier–transform infrared (FTIR) spectroscopy. ANOVA analysis was conducted to assess the significance of different factors, with *p*–values below 0.05 considered statistically significant. The obtained *F*–values, compared to *F*–crit values, indicated the overall significance of the tests. The kinetic data agreed with the Polymath Mass Transfer (PMT) model, which accurately captured the adsorption behaviour. The PMT model precisely predicted the adsorption surface area (a_m) as 612.60 m^2/g, closely aligning with the actual mesopores surface area of 547.85 m^2/g for the MB dye. Conversely, the PMT model for the MR dye failed to match the actual calculation, suggesting that the MR dye exhibited unfavourable adsorption characteristics towards PineAC. This demonstrated the reliability and robustness of the PMT model in describing the adsorption process. Exploring the potential functionalization of PineAC could offer opportunities for enhanced performance and broader applications in sustainable wastewater treatment.

Keywords: polymath mass transfer, activated carbon, mass transfer, methylene blue, methyl red

Abstrak

Kajian ini memberi tumpuan kepada penggunaan karbon teraktif kulit nanas (PineAC), dihasilkan melalui kaedah yang murah dan mesra alam, untuk penjerapan pewarna metilena biru (MB) dan metil merah (MR). PineAC telah dicirikan menggunakan pelbagai teknik seperti analisis permukaan, mikroskopi imbasan elektron (SEM), sinar–X tersebar tenaga (EDX), dan spektroskopi inframerah transformasi Fourier (FTIR). Analisis ANOVA telah dijalankan untuk menilai kepentingan faktor–faktor berbeza, dengan nilai p yang kurang daripada 0.05 dianggap signifikan secara statistik. Nilai F yang diperoleh, berbanding dengan nilai *F*–kritikal, menunjukkan kepentingan keseluruhan ujian tersebut. Data kinetik selari dengan model pemindahan jisim polimat (PMT), yang menggambarkan dengan tepat tingkah laku penjerapan. Selain itu, model PMT secara tepat meramalkan kawasan permukaan

penjerapan (a_m) sebagai 612.60 m^2/g, hampir seiring dengan kawasan permukaan mesopor sebenar 547.85 m^2/g bagi pewarna MB. Sebaliknya, model PMT bagi pewarna MR gagal sejajar dengan perhitungan sebenar, menunjukkan bahawa pewarna MR menunjukkan ciri–ciri penjerapan yang tidak menguntungkan terhadap PineAC. Ini membuktikan kebolehpercayaan dan ketahanan model PMT dalam menggambarkan proses penjerapan. Meneroka potensi pemekaan PineAC boleh memberi peluang untuk prestasi yang lebih baik dan aplikasi yang lebih luas dalam rawatan air sisa lestari.

Kata kunci: pemindahan jisim polimat, karbon teraktif, pemindahan jisim, metilena biru, metil merah

Introduction

The presence of organic dyes in industrial effluent are responsible for releasing a considerable number of dyes, including substances like methylene blue (MB) and methyl red (MR) dyes, into wastewater during synthesis and processing [1]. MB dye, for example, exhibits remarkable stability to oxidizing agents, light, and heat, due to the high intensity of its amino groups and chromophore's positive ion, making it difficult to degrade or remove from aqueous solutions [2]. The harmful effects of dyes are not limited to the environment but also extend to both human and animal forms, causing various health issues such as respiratory difficulties, nausea, eye irritation, excessive sweating, vomiting, and cognitive confusion [3–5]. Consequently, the removal of MB and MR dyes from wastewater using activated carbon (AC) is of utmost importance to prevent their release into the environment.

Pineapple peels–based AC (PineAC) as an adsorbent offers a practical approach for removing MB and MR dyes from wastewater. PineAC possesses a high surface area and porosity, providing adsorption sites for dye molecules to adhere to its surface through physical interactions such as electrostatic attraction, van der Waals forces, and π–π stacking [6]. These properties make PineAC an ideal choice for the adsorption of MB and MR dyes, facilitating their removal from wastewater prior to its discharge into the environment. The effectiveness of the adsorption process is greatly influenced by variables like temperature, pH, contact duration, and the amount of biosorbent used [7, 8]. Longer contact times and higher biosorbent dosages enhanced the adsorption capacity of AC, while an optimal pH range and temperature can promote favourable dye–biosorbent interactions [9, 8, 10]. Additionally, the mesopores in the PineAC structure can enhance its accessibility and surface area, leading to improved dyes adsorption performance [11].

In this work, mass transfer simulation improved the estimation of mesopores in PineAC structures for dyes adsorption. By employing mass transfer simulation techniques, researchers better understood the intricate processes involved in dyes adsorption within the mesopores [12]. This simulation allowed for a more accurate estimation of the mesopores' effectiveness and their contribution to the overall adsorption capacity of PineAC structures [13]. Based on the reported findings by Mohamad Yusop et al. [14–16], the observed alignment of adsorption kinetics with the mass transfer simulation using the Polymath mass transfer (PMT) model underscored the robustness and reliability in effectively describing the adsorption process. Such optimization endeavours were crucial in ensuring the judicious utilization of resources and achieving the desired level of dye removal efficacy [16]. Moreover, mass transfer simulation enabled the prediction of breakthrough behaviour in dye adsorption systems, contributing to its long–term sustainability and effectiveness [14].

In recent studies conducted by Mohamad Yusop et al. [13–16], the kinetics of dye adsorption were investigated using the PMT model for mass transfer simulation. These investigations' findings suggested that a major factor in the adsorption of dyes was the mass transfer mechanism between the biosorbent and adsorbate. Mohd Ramli et al. [13] observed that the mass transfer coefficient decreased as the initial concentration of MB dye increased when using AC biosorbent derived from the jengkol peel. In the adsorption of the remazol brilliant blue R (RBBR) dye, Mohamad Yusop et al. [14] correctly anticipated the adsorption surface area (a_m) to be 790.04 m^2/g utilizing meranti wood–based AC. This

figure was quite near the 825.58 m^2/g surface area of the mesopores. Similarly, when teak wood–based AC was employed in the adsorption of RBBR dye, the PMT model predicted the a_m value of 940.79 m^2/g, which closely aligned with the actual mesopores surface area of 983.25 m^2/g [15]. Furthermore, the PMT model successfully predicted the a_m of 807.77 m^2/g for jackfruit–based AC in the adsorption of malachite green (MG) dye, which was comparable to the actual mesopores surface area of 714.25 m^2/g with an error of 11.58% [16]. Regarding the kinetics data, the PMT model provided the best fit, and the rate constant (k_{PTM}) was found to increase from 3.96 to 4.34 h^{-1} and 4.84 to 5.22 h^{-1} as the initial RBBR dye concentration increased using meranti wood and teak wood–based AC, respectively. Conversely, jackfruit–based AC exhibited a decrease in K_{PMT} from 1.20 to 0.41 h^{-1} as the MG dye concentration increased from 25 to 300 mg/L. Overall, these studies demonstrated the significance of the PMT model in describing the kinetics of dye adsorption and the influence of various factors, such as dye concentration and biosorbent type, on the mass transfer process.

Meanwhile, ANOVA was employed to evaluate the influence of different factors on dye adsorption. Following ANOVA, post hoc Bonferroni correction analysis was conducted to thoroughly investigate the experimental groups' differences in dye adsorption capacities. This post hoc analysis allowed researchers to perform pairwise comparisons between biosorbents or conditions, identifying cases where significant differences in dye adsorption performance were observed [17]. By employing this analytical framework, valuable insights were gained regarding the relative efficacy of different biosorbents or experimental conditions, aiding in the identification of the most promising candidates for efficient dye removal.

In this study, the MB and MR dyes adsorption using PineAC was done similarly to Rosli et al. [6] work in order to understand the mass transfer simulation and statistic approach studies in adsorption studies. The PineAC was characterized using a surface analyser, Fourier Transform Infrared (FTIR), Energy Dispersive X–ray (EDX), and scanning electron microscopy (SEM). The equilibrium isotherm of PineAC–MB and PineAC–MR dyes adsorption based on different temperatures were also discussed. The study introduced the Polymath mass transfer (PMT) model for the analysis of kinetic data in the PineAC–MB and PineAC–MR dyes adsorption system, representing a novel approach. In comparison to the traditional pseudo–first–order (PFO) and pseudo–second–order (PSO) kinetic models, the PMT model offered distinct advantages, notably its capability to predict the specific surface area implicated in the adsorption process. This characteristic of the PMT model provided researchers with valuable insights, further enriching their comprehension of the underlying adsorption mechanism. By repurposing pineapple peel, disposal costs can be minimized, and the environmental impact of waste accumulation can be reduced.

Materials and Methods

Materials

The studies of the PineAC were determined using 4–dimethylaminoazobenzene–2–carboxylic acid (MR) and 3,7–bis(dimethylamino)phenazathionium chloride (MB) (82%), purchased from Sigma–Aldrich (M) Sdn. Bhd., Malaysia. Potassium hydroxide (KOH) pellets (85%) were procured from Merck in Germany. For pH adjustments during the experiment, hydrochloric acid (HCl)(37%) and sodium hydroxide (NaOH) (99%) were acquired from Merck and Essex, respectively.

Preparation of PineAC and instrumental analysis

The raw material for PineAC, known as pineapple peel, was sourced from Parit Buntar, Perak, Malaysia. To prepare the pineapple peel raw material, it underwent a washing process and was subsequently dried in an oven for two hours, as described by Iamsaard et al. [18] study. The PineAC preparation method employed in this study was a two–step pyrolysis process based on the work conducted by Rosli et al. [6, 8, 10]. The work optimized the conditions for PineAC preparation, and these optimal conditions were used in the current study. The optimal parameters included an impregnation ratio (IR) of 3.0, a carbonization temperature of 732 °C, and a carbonization duration of 1.96 hours, which represented the weight ratio of KOH to char. These specific parameters were chosen based on their ability to yield

PineAC samples with suitable properties and achieved optimal adsorption performance, as demonstrated in the findings of Rosli et al. [6]. Figure 1 illustrates the process of PineAC preparation, which involves the steps mentioned above. PineAC's characteristics were studied using suitable analytical techniques similar to Rosli et al. [6, 8].

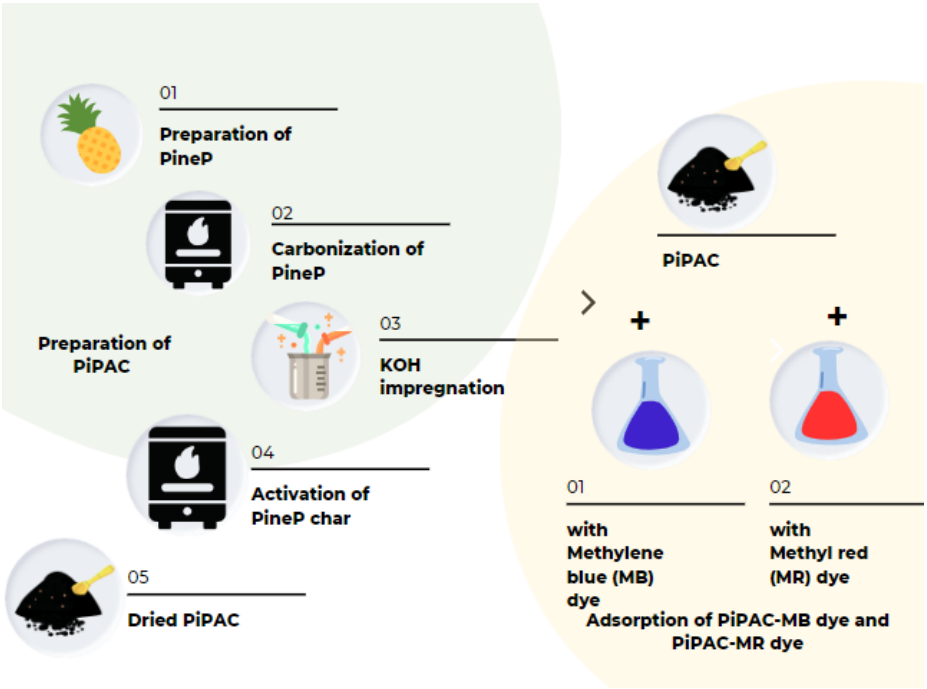

Figure 1. The flowchart for the PineAC preparation process

Adsorption studies

The batch adsorption experiments were conducted based on the methodology described in the works of Rosli et al. [6, 8]. The MB and MR dyes' maximum wavelength was 664 nm and 410 nm, respectively (Figure S1 and S2). In order to investigate the effects of initial adsorbate concentration and contact time on the adsorption process, various initial concentrations ranging from 25 to 300 mg/L for both MB and MR dyes were prepared, and the experiments were conducted over 24 hours. The impact of solution pH on the adsorption process was explored by adjusting the initial pH of the solutions within the range of 2 to 12. Furthermore, the influence of solution temperature on adsorption was investigated by conducting experiments at three different temperatures: 30, 45, and 60 °C.

Results and Discussion

Characterization of PineAC

PineAC exhibited a significant BET surface area of 1160 m^2/g. With an average pore diameter of 2.17 nm and a surface area of 547.85 m^2/g, PineAC's mesoporous character was evident [6]. The increased pore volume and surface area of PineAC were attributed to the removal of volatile matter and moisture content during the carbonization and pyrolysis of pineapple peel raw material (Figure 2(a)) [6–8]. As a result, the overall pore volume of PineAC increased from 0.173 cm^3/g to 0.544 cm^3/g. This is due to the carbonization process effectively enlarging the average pore width in the mesoporous regions [5]. The surface morphology of PineAC is shown in Figure 2(b), which highlights an uneven, sizable pore structure on the surface. The heterogeneous pore structure of PineAC was able to grow thanks to the KOH impregnation. The physiochemical treatment that created porous PineAC

enhanced the adsorption capability of MB and MR dyes [19].

The EDX analysis (Figure 2(c)) showed that the PineAC consisted of 0.14% sulphur, 67.18% carbon, 14.05% oxygen, 12.79% N_2, 4.62% potassium, 0.44% magnesium, and 0.79% calcium, implying that it was a specific sort of AC created by heating carbonaceous materials in the presence of a chemical agent [8]. Figure 2(d) shows the FTIR spectra of PineAC, revealing multiple peaks corresponding to various functional groups. The O–H stretching of the hydroxyl group appeared in the wavelength range of 3865-3610 cm^{-1}. The C≡C stretching of the alkyne group was observed within the range of 2399-2094 cm^{-1}. The presence of the C=O stretching in aldehydes and ketones was indicated by a characteristic peak at approximately 1732 cm^{-1}. Furthermore, the C=C stretching of the aromatic group generated a distinct peak at around 1527 cm^{-1}. Lastly, the =C–H bend of alkenes contributed to the spectrum by exhibiting a peak around 991 cm^{-1}. These specific wavelength ranges provided valuable insights enabling its identification and characterization in MB and MR dye removal [6,16].

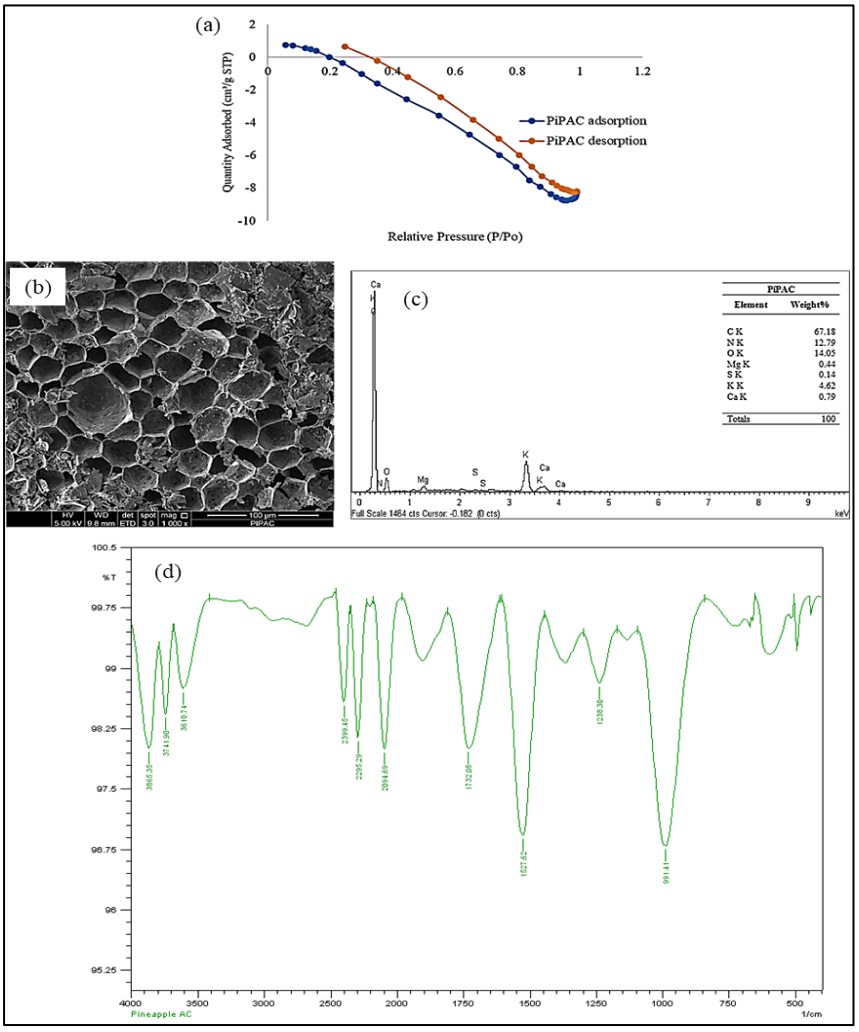

Figure 2. (a) N_2 adsorption/desorption isotherm, (b) SEM image, (c) EDX spectra, and (d) the FTIR spectrums of PineAC

Batch adsorption studies and statistical analysis

The adsorption capacity (q_t) for PineAC–MB dye increased from 23.993 to 165.177 mg/g as the starting concentration increased to 300 mg/L at 60 °C (Figure 3(a)). Initial MB dye concentrations ranging from 25 to 100 mg/L were observed to reach equilibrium more quickly (< 5 hours) compared to between 20 to 24 hours. This can be attributed to a lower ratio of MB dye to available sites, allowing for efficient adsorption at lower concentrations. However, the removal of MB dye (%) decreased at higher concentrations due to the larger ratio of MB dye to accessible sites. This removal efficiency decrease occurred because many PineAC surface sites were initially accessible for adsorption [5, 19]. Similarly, in Figure 3(b), the adsorption uptakes of PineAC–MR dye at equilibrium increased from 14.48 to 94.870 mg/g as the starting concentration was raised from 25 to 300 mg/L. This can be attributed to a stronger mass transfer force driving greater uptake of MR dye at higher concentrations. The presence of other adsorbate species in the solution and the delayed diffusion of solute molecules into the bulk of the biosorbent were additional contributing factors [8]. Furthermore, at 60 °C, the amount of MB dye adsorbed rose from 129.77 mg/g to equilibrium, while the adsorption uptakes of PineAC–MR dye increased from 54.85 mg/g (Figure 3(d)). The rate of adsorbate molecule diffusion into the internal pores of the biosorbent particles and across the external boundary layer was accelerated by the rise in temperature [6, 19].

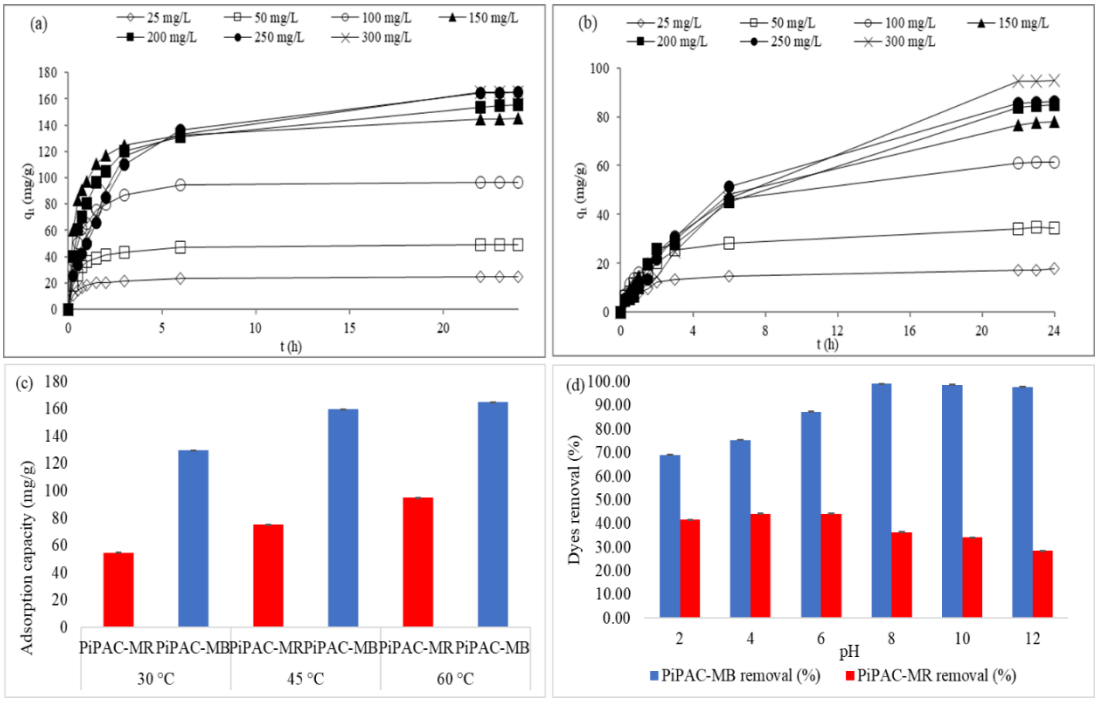

Figure 3. The q_t of (a) PineAC–MB dye and (b) PineAC–MR dye were measured at 60°C within 24 hours (25 to 300 mg/L). The effect of (c) temperature and (d) pH on PineAC–MB and PineAC –MR dyes were also shown

Based on the data presented in Figure 3(d), it was observed that the removal of PineAC–MB dye increased with an increase in pH in the solution. The maximum removal of PineAC–MB dye, reaching 99%, was achieved at pH 8. Moreover, the adsorption of MB dye remained relatively constant above pH 8. At low pH levels, the low adsorption of PineAC–MB dye was attributed to the abundance of H^+ ions competing with the MB dye cation for adsorption sites on the PineAC surface. Conversely, the negatively charged PineAC surface exhibited an attractive electrostatic force at high pH levels, promoting the elevation and adsorption of the positively charged MB dye cation [6]. On the other hand, PineAC–MR dye adsorption displayed a

preference for an acidic environment, with optimal adsorption observed at pH 6. This can be attributed to the abundance of positively charged PineAC sites under acidic conditions, facilitating the adsorption of MR dye. Additionally, as the pH rose above 6, there were more negatively charged sites. The increased adsorption of MR dye with a drop in pH value was explained by the attraction between the azo dye and more H^+ ions in the solution [8, 10].

Because of its azo group–based chemical structure, MR dye had lower adsorption uptakes than PineAC–MB dye. However, MB dye, a basic dye, has cationic properties because of its positive charge, which was frequently dispersed throughout the chromophoric system [20]. Notably, PineAC shared the same hexatomic ring of carbon atoms (Figure 4), enabling it to naturally form π–π interactions with both MB and MR dyes. Due to reduced electrostatic interactions, this showed that van der Waals forces were more important than hydrogen bonding in preserving the stability of the complex [8, 10]. These results suggested that the intensity and frequency of van der Waals interactions within the system affected the binding of PineAC with MB and MR dyes as well as the consequent adsorption capacities and overall stability. These results suggested that the intensity and frequency of van der Waals interactions within the system affected the binding of PineAC with MB and MR dyes as well as the consequent adsorption capacities and overall stability.

The ANOVA test was a statistical tool utilized to assess significant differences among the means of multiple groups in this study. In the context of adsorption studies, ANOVA analysis enabled the investigation of various factors' impacts on the adsorption process and determined their statistical significance [21]. ANOVA tests were conducted to evaluate the significance of four primary adsorption parameters, temperature, initial dye concentration, pH, and contact time, on the PineAC with MB and MR adsorption. The influential factors were identified by examining the statistical significance of these variables, and their effects on the adsorption process were understood. The variables in this study were defined as contact time (24 hours), initial dye concentration (25-300 mg/L), pH (2-12), and temperature (30-60 °C). The summary statistical analysis in Table 1 presented the effects of major interactive variables, including degrees of freedom (df), *F*–values, *F*-crit, sum of squares (SS), mean square (MS), and *p*–values. A *p*–value below 0.05 indicated the significance of the models in the regression analysis considering the independent variables. The analysis of the ANOVA models was conducted by assessing the significance of each term, considering *p*–values below 0.05 as statistically significant. The larger *F*–values compared to *F*-crit values indicated the overall significance of the tests. Consequently, these statistical outcomes supported the acceptance of the alternative hypothesis, suggesting significant differences between the means of the analysed parameters.

However, as the ANOVA test alone does not provide specific information regarding the significant differences between individual parameters, a post–hoc test with Bonferroni correction was conducted to analyse the data further. Table 2 presents a summary of the Post–Hoc Tests (Bonferroni Correction) conducted to assess the effects of temperature, initial dye concentration, and pH on the adsorption of PineAC–MB and PineAC–MR dyes [22]. The *t*–test with adjusted *p*–values were performed for each parameter, and the Bonferroni correction method was employed to account for multiple comparisons. By adjusting the alpha level (0.05) based on the provided data, the likelihood of Type I errors resulting from multiple hypothesis testing was effectively controlled. The analysis yielded significant results, as evidenced by the calculated adjusted *p*–values. Specifically, for PineAC–MB dye, statistically significant differences were observed between contact time and initial dye concentrations of 100-300 mg/L, as well as between pH and dye removal (%). In the case of PineAC–MR dye, all combinations of initial dye concentration, contact time, and pH, with the percentage of dye removal, were found to be statistically significant. These findings further underscore the significance of the analysed parameters and offer more comprehensive insights into their respective effects on the adsorption process.

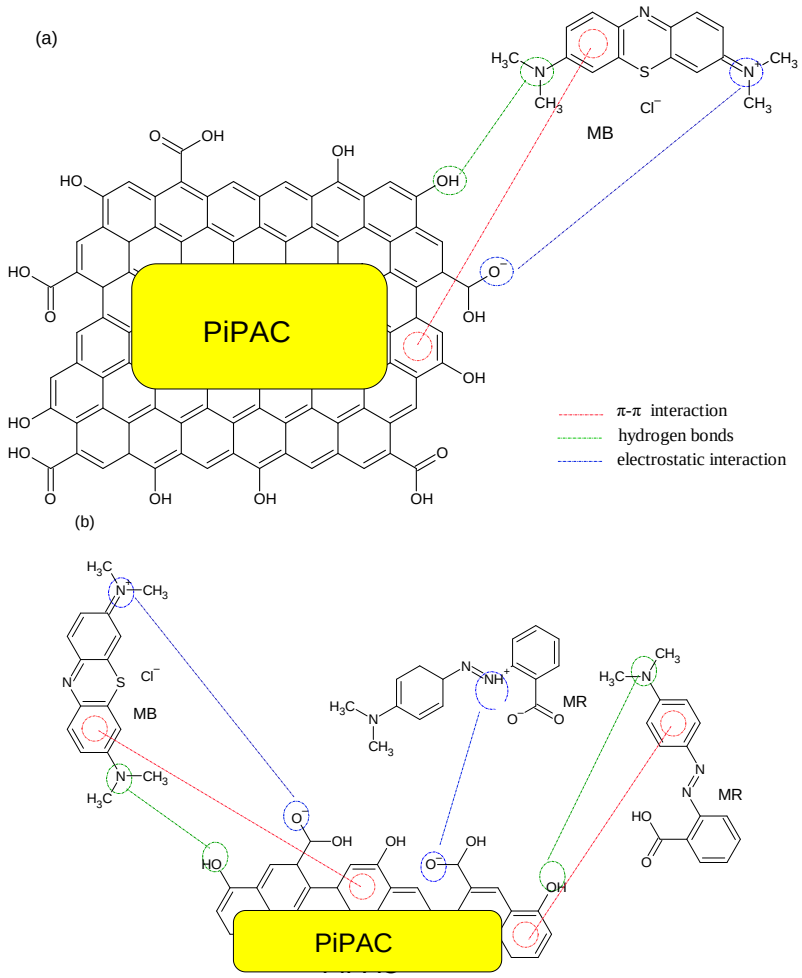

Figure 4. The mechanism of (a) PineAC–MB and (b) PineAC–MR dyes adsorption

Adsorption isotherm studies

In this study, the Langmuir and Freundlich isotherm models were selected to analyse the experimental equilibrium data. Figure S3 illustrates the adsorption equilibrium curves obtained from each isotherm model and compares them with the experimental values for PineAC–MB and PineAC–MR dyes at 30 to 60 °C. The goodness of fit for each model was assessed based on the R^2 values, as shown in Table 3. The Langmuir isotherm model exhibited in agreement with the experimental data ($R^2 > 0.99$) for the adsorption of both PineAC–MB and PineAC–MR dyes at 60 °C. The Langmuir model suggested a monolayer adsorption behaviour, and the maximum adsorption capacities (Q_m) were determined as 168.528 mg/g and 107.798 mg/g for PineAC–MB and PineAC–MR dyes, respectively [6]. On the other hand, the Freundlich isotherm parameters showed that the adsorption process for PineAC–MB and PineAC–MR dyes was favourable at 30 to 45 °C. The Freundlich model describes a physical adsorption process and provides information about the heterogeneity and adsorption intensity of the biosorbent [23]. The results indicated that PineAC demonstrated favourable adsorption characteristics for both PineAC–MB and PineAC–MR dyes. The Langmuir model represented the monolayer adsorption behaviour at 60 °C, while the Freundlich model confirmed the favourable physical adsorption process at lower temperatures.

Table 1. The summary of ANOVA analysis for the effect of temperature, initial dye concentration, and pH for PineAC–MB and PineAC–MR dyes adsorption

PineAC–MB dye							PineAC–MR dye						
Source of Variation	**SS**	**df**	**MS**	**F**	**P–value**	**F crit**	**Source of Variation**	**SS**	**df**	**MS**	**F**	**P–value**	**F crit**
Initial concentration of dye and contact time													
Regression	659482.87	8	82435.36	78.2587	1.9412E–36	2.0467	Regression	796445.72	8	99555.72	145.7884	5.1016E–47	2.0467
Residual	91643.18	87	1053.37				Residual	59410.39	87	682.88			
Effect of temperature													
Regression	120244.13	7	17177.73	10.9740	6.874E–10	2.1155	Regression	10544.06	7	1506.29	2.2321	0.0389	2.1155
Residual	137746.87	88	1565.31				Residual	59385.62	88	674.84			
Effect of pH													
Regression	15704.99	1	15704.99	141.5461	3.1672E–07	4.9646	Regression	5019.404	1	5019.40	178.9319	1.0456E–07	4.9646
Residual	1109.53	10	110.95				Residual	280.5203	10	28.05			

Table 2. The summary of Post–Hoc Tests (Bonferroni Correction) for the effect of initial dye concentration, temperature, and pH for PineAC–MB and PineAC–MR dyes adsorption

PineAC–MB dye				PineAC–MR dye			
Initial concentration of dye and contact time							
Groups (min vs. mg/L)	**t–test (new p–value)**	**Significant**	**Post–Hoc Tests (Bonferroni Correction) alpha**	**Groups (min vs. mg/L)**	**t–test (new p–value)**	**Significant**	**Post–Hoc Tests (Bonferroni Correction) alpha**
time vs. 25	0.4134	NO		time vs. 25	1.0184E–03	YES	
time vs. 50	0.0190	NO		time vs. 50	4.0421E–08	YES	
time vs. 100	0.0002	YES		time vs. 100	4.3543E–13	YES	
time vs. 150	2.701E–07	YES	0.0063	time vs. 150	6.3070E–17	YES	0.0063
time vs. 200	1.678E–10	YES		time vs. 200	2.0634E–19	YES	
time vs. 250	1.056E–12	YES		time vs. 250	2.6235E–20	YES	
time vs. 300	3.289E–14	YES		time vs. 300	1.4000E–21	YES	
Effect of temperature							
Groups	**t–test (new p–value)**	**Significant**	**Post–Hoc Tests (Bonferroni Correction) alpha**	**Groups**	**t–test (new p–value)**	**Significant**	**Post–Hoc Tests (Bonferroni Correction) alpha**
concentration vs. 30°C	0.1721	NO		concentration vs. 30°C	0.0125	YES	
concentration vs. 45°C	0.3257	NO	0.0167	concentration vs. 45°C	0.0222	NO	0.0167
concentration vs. 60°C	0.3968	NO		concentration vs. 60°C	0.0490	NO	
Effect of pH							
Groups	**t–test (new p–value)**	**Significant**	**Post–Hoc Tests (Bonferroni Correction) alpha**	**Groups**	**t–test (new p–value)**	**Significant**	**Post–Hoc Tests (Bonferroni Correction) alpha**
pH vs. removal %	3.1672E–07	YES	0.0250	pH vs. removal %	1.0456E–07	YES	0.0250

Table 3. Isotherm parameters for PineAC–MB and PineAC–MR dyes adsorption

T (°C)	PineAC–MB dye				PineAC–MR dye			
	Langmuir		Freundlich		Langmuir		Freundlich	
30	Q_m	128.529	K_F	46.457	Q_m	58.552	K_F	8.02
	K_L	0.266	n_F	4.747	K_a	0.03	n_F	2.853
	R^2	0.986	R^2	0.991	R^2	0.72	R^2	0.877
	Δq_e (%)	0.72	Δq_e (%)	16.799	Δq_e (%)	0.53	Δq_e (%)	1.561
45	Q_m	160.119	K_F	58.486	Q_m	86.794	K_F	8.153
	K_a	0.287	n_F	4.695	K_a	0.02	n_F	2.451
	R^2	0.885	R^2	0.999	R^2	0.969	R^2	0.997
	Δq_e (%)	2.097	Δq_e (%)	20.549	Δq_e (%)	1.068	Δq_e (%)	1.481
60	Q_m	168.528	K_F	77.152	Q_m	107.798	K_F	13.942
	K_a	0.524	n_F	5.804	K_a	0.032	n_F	2.706
	R^2	0.975	R^2	0.974	R^2	1	R^2	0.948
	Δq_e (%)	15.353	Δq_e (%)	13.522	Δq_e (%)	0.432	Δq_e (%)	7.593

The studies discussed highlighted the diverse applications of pineapple peel and its derivatives as effective biosorbents for pollutant removal. These findings contributed significantly to the field of water and wastewater treatment, showcasing the potential of pineapple–based materials. To further contextualize and add depth to these discussions, a comparative analysis with existing literature and a focus on the novelty of the PineAC biosorbent was elucidated. Comparative studies with existing literature revealed the uniqueness of PineAC in terms of its adsorption capacities. While Ugbe et al. [24] and Chaiyaraksa et al. [25] reported q_{max} values for the removal of Eosin Yellow and Basic Red 9 using untreated pineapple peel, the development of PineAC surpassed these capacities. PineAC achieved a remarkable q_{max} of 165.17 mg/g at pH 8 for the removal of a pollutant, exceeding the reported values in previous studies [22]. This significant enhancement in adsorption capacity could be attributed to the specific activation methods and processing techniques employed in the synthesis of PineAC, setting it apart from traditional pineapple peel–based biosorbents.

The utilization of pineapple peel for hydrogel development, as demonstrated by Dai et al. [26], showcased high adsorption capacities for Congo Red removal. However, PineAC outperformed these hydrogels, achieving a q_{max} of 165.17 mg/g compared to the reported values of 114.940 mg/g for water pineapple peel hydrogels. The alkali and bleaching pineapple peel hydrogels also demonstrated lower q_{max} values of 77.520 mg/g and 138.890 mg/g, respectively. This suggested that the specific formulation and activation process of PineAC contributed to its superior adsorption performance. Activation methods played a crucial role in enhancing the adsorption capacity of biosorbents. While Turkmen et al. [27] activated pineapple peel using $ZnCl_2$ and observed an increased q_{max} for the adsorption of Zn(II), the PineAC biosorbent, activated through a different method, achieved a higher q_{max} at 165.17 mg/g. Similarly, the H_2SO_4–activated pineapple peel showed promise with a q_{max} of 36.99 mg/g, but PineAC surpassed this capacity, indicating the effectiveness of the novel activation method used in its synthesis.

Furthermore, the comparative analysis extended to the temperature–dependent biochar production process explored by Shakya and Agarwal [28]. Pineapple peel biochar exhibited q_{max} values ranging from 23.81 to 33.33 mg/g for Cr(VI) adsorption. In contrast, PineAC demonstrated a significantly higher q_{max} of 165.17 mg/g at pH 8, highlighting the superiority of PineAC for pollutant removal. The investigation of pineapple peel for Cd(II) removal by Yusoff et al. [29] reported a q_{max} of 1.91 mg/g. In comparison, PineAC showcased a substantially higher adsorption capacity of 165.17 mg/g at pH 8. This emphasized the versatility of PineAC across a broad spectrum of pollutants and pH conditions, and its efficacy in comparison to conventional pineapple peel–based biosorbents.

Thus, the presented comparative discussion emphasizes the pioneering nature of the PineAC biosorbent. The innovative approach to activation and processing techniques led to a significant enhancement in adsorption capacities, outperforming existing literature across various pollutants and pH conditions. The development of PineAC opened new avenues for sustainable and efficient solutions in water and wastewater treatment, showcasing its potential as a leading biosorbent in the field. Further research and optimization of PineAC and similar derivatives held promise for advancing the landscape of environmental remediation technologies.

Table 4. Comparative analysis of the adsorption capacity of pineapple peel adsorbate based on different pollutant

Adsorbent Name	q_{max} (mg/g)	pH	Pollutant	Ref.
Pineapple peel as biosorbents	11.76	–	Eosin Yellow	[24]
Pineapple peel activated by $ZnCl_2$	37.23	–	Zn(II)	[27]
Pineapple peel activated by H_2SO_4	36.99	–		
Silver nanoparticles from pineapple peel waste	98.04	9.96	MB	[22]
Pineapple peel biochar	23.81–33.33	2	Cr(VI)	[28]
Pineapple peel	11.389	7	Basic Red 9	[25]
Water pineapple peel hydrogels	114.94	4	Congo Red	[26]
Alkali pineapple peel hydrogels	77.52			
Bleaching pineapple peel hydrogels	138.89			
Pineapple peel	1.91	9	Cd(II)	[29]
PineAC	165.17	8	MB	This work
	94.87	6	MR	

Adsorption kinetic studies and mass transfer simulation

This study utilized three kinetic models: the PFO, PSO, and PMT models. The PFO and PSO models' q_e (mg/g) values showed a rise with increasing starting concentration, from 25 to 300 mg/L at 30 to 60 °C (supplementary data). This trend indicated that as the initial concentrations of MB and MR dyes increased, the adsorption capacity of PineAC also increased, suggesting a stronger affinity between the MB and MR dye molecules and the adsorption sites on PineAC [6]. Comparing the two models, the PSO kinetic model demonstrated higher consistency regarding R^2 and Δq_t values than the PFO model. Additionally, the k^2 value showed a non–linear pattern with increasing initial concentration, suggesting the influence of various mechanisms on the adsorption of PineAC–MB and PineAC–MR dyes.

Table 5 summarizes the kinetic parameters based on different temperatures for PFO, PSO, and PMT, showing relatively high average R^2 values at 30 to 60°C. However, for PineAC–MB dye adsorption, both the PFO and PSO models exhibited relatively high average Δq_t percentages, ranging from 29.01 to 72.59% and 6.55 to 77.12%, respectively, at 30 to 60°C. Similarly, for PineAC–MR dye adsorption, the PFO and PSO models showed relatively low average Δq_t percentages, ranging from 5.50 to 54.11% and 60.82 to 26.96%, respectively, compared to PineAC–MB dye adsorption. These percentages suggested that these models were not able to accurately predict the uptake of PineAC–MB and PineAC–MR dyes at equilibrium, $q_{e,\,cal}$ [13]. In contrast, the PMT model of PineAC–MB and PineAC–MR dyes adsorption demonstrated relatively low average Δq_t percentages of 1.3526 to 1.53% and 0.36 to 1.01%, respectively, at 30 °C to 60 °C, indicating the best fit for the kinetic data.

Moreover, the PMT model (Figures 5 and 6) accurately predicted the highest adsorption surface area to be 612.60 m^2/g (with an error percentage of 1.35%) for the MB dye, closely matching the actual mesopores surface area of 547.85 m^2/g [14]. However, the PMT model for the MR dye showed the highest adsorption surface area of 192.55 m^2/g (with an error percentage of 0.41%) and was unable to correspond to the actual mesopores surface area. This discrepancy was likely due to the low percentage of removal of the MR dye by PineAC, making it less favourable for adsorption. The investigated study explored the relationship between the initial concentrations of MB and MR dyes and mass transfer rates, with a focus on the formation of concentration gradients and the resulting mass transfer driving force [15]. Further analysis revealed that as the initial concentrations of MB and MR dyes increased from 25 mg/L to 300 mg/L, the PMT $q_{e,\ exp}$, and $q_{e\ cal}$ exhibited similar values and increased at 30 to 60°C. Generally, higher initial concentrations of MB and MR dyes resulted in more significant concentration gradients, leading to a more substantial mass transfer driving force. Consequently, this relationship typically led to higher rate constants and increased mass transfer rates [16].

Table 5. The summary of the kinetic model for PFO, PSO, and PMT constant parameters of PineAC–MB and PineAC–MR dyes adsorption at 30 to 60°C

T (°C)	Kinetic Parameters	PineAC–MB Dye			PineAC–MR Dye		
		PFO	PSO	PMT	PFO	PSO	PMT
30	a_{PMT} (m^2/g)	–	–	233.6181	–	–	66.3993
	R^2	0.9609	0.9556	0.9724	0.9414	0.9243	0.9908
	Δq_t (%)	35.3653	10.7867	1.3526	13.3754	26.9687	0.3645
45	a_{PMT} (m^2/g)	–	–	307.4033	–	–	44.1481
	R^2	0.9657	0.9666	0.9695	0.9389	0.8521	0.9453
	Δq_t (%)	72.5954	77.1249	1.5319	54.1171	16.9886	1.0175
60	a_{PMT} (m^2/g)	–	–	612.6089	–	–	192.5528
	R^2	0.9561	0.9366	0.9763	0.9701	0.7047	0.9932
	Δq_t (%)	29.0193	6.5549	1.3528	5.5066	0.8211	0.4190

Conclusion

The physiochemical treatment employed during the production of PineAC resulted in the formation of a porous structure, significantly enhancing its adsorption capacity for MB and MR dyes. The observed surface morphology was consistent with N_2 adsorption isotherm, EDX, and FTIR analysis. The ANOVA models indicated statistically significant differences (*p*–values <0.05), and the larger *F*–values compared to *F*–crit values supported the acceptance of the alternative hypothesis, suggesting significant differences between the means of the analysed parameters. In–depth, kinetic studies revealed that the PMT model provided the best fit for the investigated adsorption system. Notably, the PMT model accurately predicted the MB dye adsorption surface area to be 612.60 m^2/g, closely matching the measured value of PineAC's mesopores surface area. This high level of precision underscores the reliability and accuracy of the PMT model in describing the adsorption process. These findings highlight the potential of PineAC as an efficient and cost–effective adsorption system for the removal of MB and MR dyes. Further research and development in this direction can contribute to the advancement of PineAC–based adsorption systems for effective dye removal.

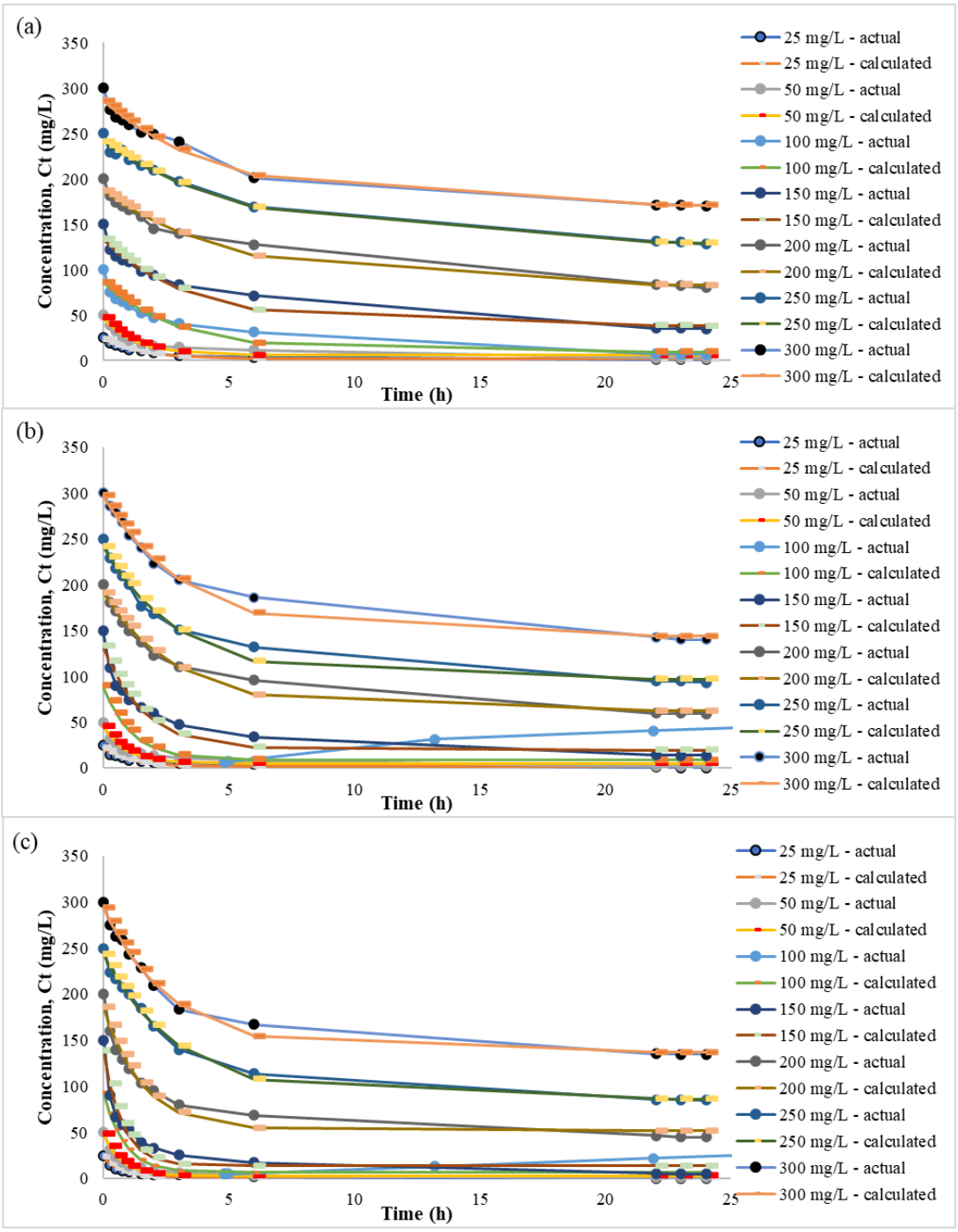

Figure 5. PMT model graphs for adsorption of PineAC–MB dye at (a) 30, (b) 45, and (c) 60°C

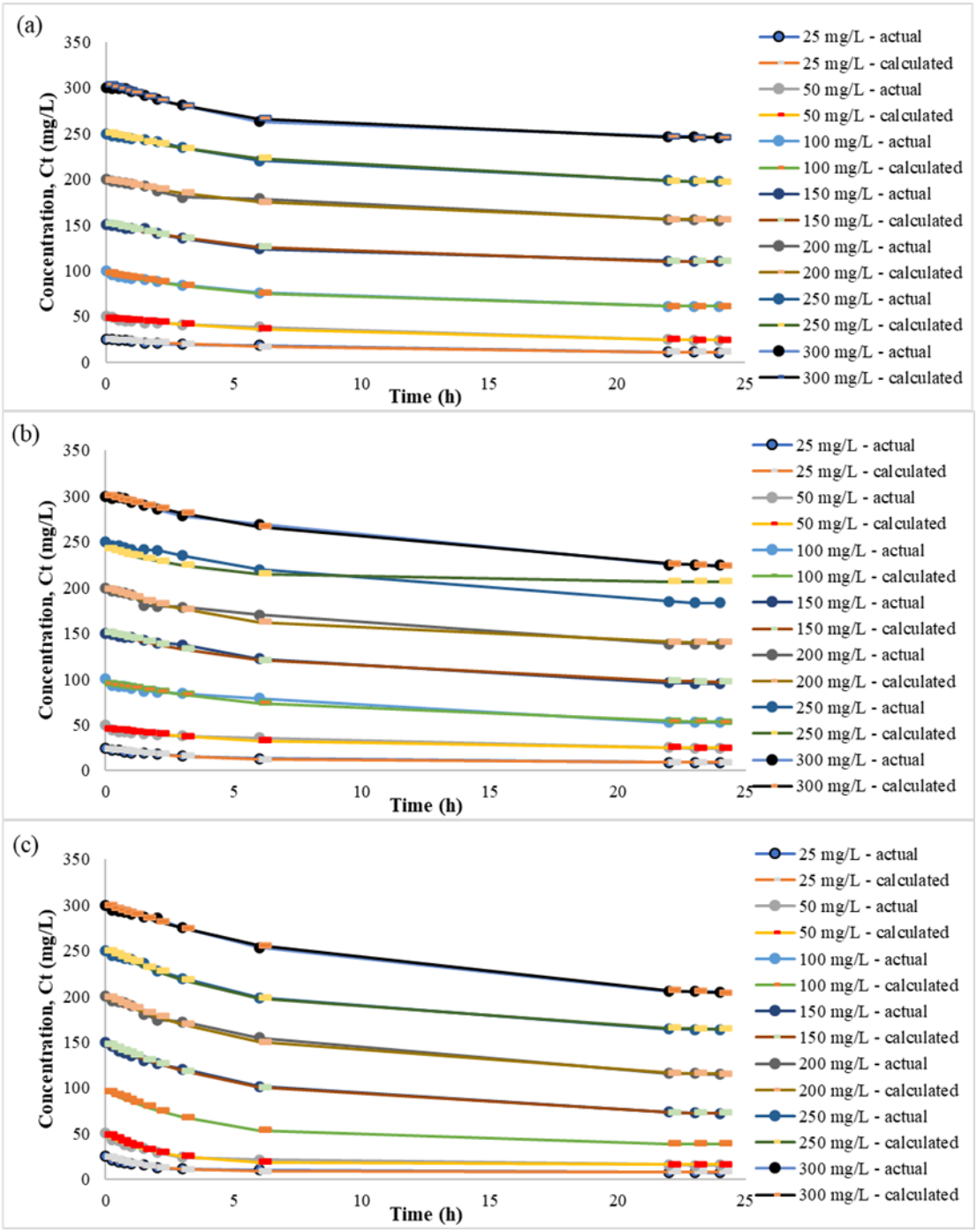

Figure 6. PMT model graphs for adsorption of PineAC–MR dye at (a) 30, (b) 45, and (c) 60°C

Acknowledgements

The authors express their sincere gratitude to Short Term Grant (Grant no. 6315463) from Universiti Sains Malaysia for their support and enabling the advancement of knowledge in this field of study.

References

1. Bilal, M., Ali, J., Bibi, K., Khan, S. B., Saqib, M., Saeed, R., Javeria, R., H. Khan, H., Akhtar, K. and Bakhsh, E. M. (2022). Remediation of different dyes from textile effluent using activated carbon

synthesized from *Buxus Wallichiana*. *Industrial Crops and Products,* 187 (Part A): 115267.

2. Jabar, J. M., Odusote, Y. A., Ayinde, Y. T. and Yılmaz, M. (2022). African almond (*Terminalia catappa L.*) leaves biochar prepared through pyrolysis using H_3PO_4 as chemical activator for sequestration of methylene blue dye. *Results in Engineering,* 14: 100385.
3. Mahmad A., Noh T. U., Khalid N.I. (2023). Eco–friendly water treatment: The role of MIL metal–organic frameworks for the bisphenols adsorption from water. *Inorganic Chemistry Communications,* 152: 110643.
4. Kuśmierek, K., Świątkowski, A., Kotkowski, T., Cherbański, R., Molga, E. (2021). Adsorption on activated carbons from end–of–life tyre pyrolysis for environmental applications. Part II. Adsorption from aqueous phase. *Journal of Analytical and Applied Pyrolysis,* 158: 105206.
5. Ahmad, M. A., Eusoff, M. A., Adegoke, K. A. and Bello, O. S. (2021). Sequestration of methylene blue dye from aqueous solution using microwave assisted dragon fruit peel as adsorbent. *Environmental Technology & Innovation,* 24: 101917.
6. Rosli, N. A., Ahmad, M. A., Noh, T. U. (2023). Unleashing the potential of pineapple peel–based activated carbon: response surface methodology optimization and regeneration for methylene blue and methyl red dyes adsorption. *Inorganic Chemistry Communications,* 2023: 111041.
7. Khasri, A. and Ahmad, M. A. (2018). Adsorption of basic and reactive dyes from aqueous solution onto *Intsia bijuga* sawdust–based activated carbon: batch and column study. *Environmental Science and Pollution Research,* 25: 31508-31519.
8. Rosli, N. A., Ahmad, M. A., Noh, T. U. and Ahmad, N. A. (2023). Pineapple peel–derived carbon for adsorptive removal of dyes. *Materials Chemistry and Physics,* 2023: 128094.
9. Khasri, A., Mohd Jamir, M. R., Ahmad, A. A. and Ahmad, M. A. (2021). Adsorption of Remazol Brilliant Violet 5R dye from aqueous solution onto melunak and rubberwood sawdust based activated carbon: interaction mechanism, isotherm, kinetic and thermodynamic properties. *Desalination and Water Treatment,* 216: 401-411.
10. Rosli, N. A., Ahmad, M. A., Noh, T. U. (2023). Nature's waste turned saviour: Optimizing pineapple peel–based activated carbon for effective Remazol Brilliant Violet dye adsorption using response surface methodology. *Inorganic Chemistry Communications* 153: 110844.
11. Aragaw, T. A. and Bogale, F. M. (2021). Biomass–based adsorbents for removal of dyes from wastewater: A review. *Frontiers in Environmental Science,* 9: 764958.
12. Inglezakis, V. J., Balsamo, M. and Montagnaro, F. (2020). Liquid–solid mass transfer in adsorption systems—an overlooked resistance?. *Industrial & Engineering Chemistry Research,* 59(50): 22007-22016.
13. Mohd Ramli, M. R., Shoparwe, N. F., Ahmad, M. A. (2022). Methylene blue removal using activated carbon adsorbent from Jengkol Peel: Kinetic and mass transfer studies. *Arabian Journal of Science and Engineering,* 48: 8585-8594.
14. Mohamad Yusop, M. F., Tamar Jaya, M. A., Idris, I., Abdullah, A. Z. and Ahmad, M. A. (2023). Optimization and mass transfer simulation of remazol brilliant blue R dye adsorption onto meranti wood based activated carbon. *Arabian Journal of Chemistry,* 16(5): 104683.
15. Mohamad Yusop, M. F., Nasehir Khan, M. N., Zakaria, R., Abdullah, A. Z., Ahmad, M. A. (2023). Mass transfer simulation on Remazol Brilliant Blue R dye adsorption by optimized teak wood based activated carbon. *Arabian Journal of Chemistry,* 16: 104780.
16. Mohamad Yusop, M. F., Abdullah, A. Z. and Ahmad, M. A. (2023). Malachite green dye adsorption by jackfruit based activated carbon: Optimization, mass transfer simulation, and surface area prediction. *Diamond and Related Materials,* 136: 109991.
17. Nandiyanto, A. B. D., Girsanga, G. C. S., Maryanti, R., Ragadhitaa, R., Anggraenia, S., Fauzia, F. M., Sakinaha, P., Astutia, A. P., Usdiyana, D., Fiandinia, M., Dewi, M. W. and Al–Obaidi, A. S. M. (2020). Isotherm adsorption characteristics of carbon microparticles prepared

from pineapple peel waste. *Communications in Science and Technology,* 5(1): 31-39.

18. Iamsaard, K., Weng, C.H., Yen, L.T., Tzeng, J.H., Poonpakdee, C. and Lin, Y.T. (2022). Adsorption of metal on pineapple leaf biochar: Key affecting factors, mechanism identification, and regeneration evaluation. *Bioresource Technology,* 344: 126131.
19. Ahmad, M. A., Eusoff, M. A., Oladoye, P. O., Adegoke, K. A. and Bello, O. S. (2021b). Optimization and batch studies on adsorption of Methylene blue dye using pomegranate fruit peel–based adsorbent. *Chemical Data Collections,* 32: 100676.
20. Thi, H. T., Le Hoang, A., Huu, T. P., Dinh, T. N., Chang, S. W., Chung, W. J., Nguyen, D. D. (2020). Adsorption isotherms and kinetic modeling of methylene blue dye onto a carbonaceous hydrochar adsorbent derived from coffee husk waste. *Science of The Total Environment,* 725:138325.
21. Srivastava, A., Gupta, B., Majumder, A., Gupta, A. K. and Nimbhorkar, S. K. (2021). A comprehensive review on the synthesis, performance, modifications, and regeneration of activated carbon for the adsorptive removal of various water pollutants. *Journal of Environmental Chemical Engineering,* 9(5): 106177.
22. Agnihotri, S., Sillu, D., Sharma, G. and Arya, R. K. (2018). Photocatalytic and antibacterial potential of silver nanoparticles derived from pineapple waste: Process optimization and modelling kinetics for dye removal. *Applied Nanoscience,* 8: 2077-2092.
23. Mahmad, A., Shaharun, M. S., Noh, T. U., Zango, Z. U. and Taha, M. F. (2022). Experimental and molecular modelling approach for rapid adsorption of Bisphenol A using Zr and Fe based metal–organic frameworks. *Inorganic Chemistry Communications,* 142: 109604.
24. Ugbe, F. A., Anebi, P. O. and Ikudayisi, V. A. (2018). Biosorption of an anionic dye, eosin yellow onto pineapple peels: isotherm and thermodynamic study. *International Annals of Science,* 4(1): 14-19.
25. Chaiyaraksa, C., Ruenroeng, C., Buaphuan, B. and Choksakul, S. (2019). Adsorption of cationic and anionic dye using modified pineapple peel. *Songklanakarin Journal of Science and Technology,* 41(1): 199-206.
26. Dai, H., Huang, Y., Zhang, H., Ma, L., Huang, H., Wu, J. and Zhang, Y. (2019). Direct fabrication of hierarchically processed pineapple peel hydrogels for efficient Congo red adsorption. *Carbohydrate Polymers,* 2019: 115599.
27. Turkmen, K. S. N., Kipcak, A. S., Moroydor Derun, E. and Tugrul, N. (2021). Removal of zinc from wastewater using orange, pineapple and pomegranate peels. *International Journal Environmental Science and Technology,* 18: 2781-2792.
28. Shakya, A., T. and Agarwal, T. (2019). Removal of Cr (VI) from water using pineapple peel derived biochars: Adsorption potential and re–usability assessment. *Journal of Molecular Liquids,* 293: 111497.
29. Yusoff, A. H., Mohammad, R., Mohamad, M., Sulaiman, A.Z., Che Zaudin, N. A., Rosmadi, N., Aqsa, F., Yusoff, M. and Teo, P. (2020). Potential of agricultural waste material (*Ananas cosmos*) as biosorbent for heavy metal removal in polluted water. *Material Science Forum,* 1010: 489-494.